

High Thermal Performance of SnO₂:F Thin Transparent Heaters with Scattered Metal Nanodots

Chairul Hudaya,^{†,‡} Bup Ju Jeon,^{*,§} and Joong Kee Lee^{†,‡}

[†]Center for Energy Convergence Research, Green City Research Institute, Korea Institute of Science and Technology, Hwarangno 14-gil 5, Seongbuk-gu, Seoul 136-791, Republic of Korea

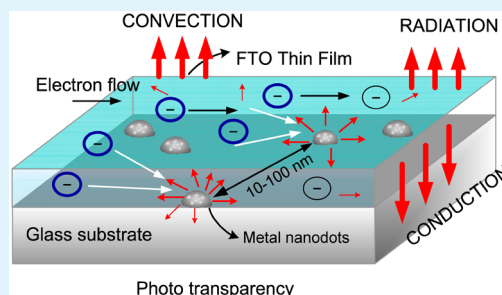
[‡]Department of Energy and Environmental Engineering, Korea University of Science and Technology, 176 Gajungro Yuseong-gu, Daejeon 305-350, Republic of Korea

[§]Department of Energy and Environmental Engineering, Shinhan University, 233-1, Sangpaedong, Dongducheon, Gyeonggi-do 483-777, Republic of Korea

S Supporting Information

ABSTRACT: Facile production and novel transparent heaters consisting of fluorine-doped tin oxide (SnO₂:F or FTO) thin films covered with three different scattered metal nanodots (Cr-nd, NiCr-nd and Ni-nd) prepared by plasma-enhanced sputtering system and electron cyclotron resonance–metal organic chemical vapor deposition are investigated. The heaters exhibit excellent optical transmittances of over 85% and superior saturated temperatures of more than 80 °C when a relatively low 12 V DC is supplied. The scattered metal nanodots FTO heaters successfully improve the specific power of bare FTO heater by 21, 15, and 12% for NiCr-nd FTO, Cr-nd FTO, and Ni-nd FTO, respectively. These results reveal that the FTO transparent heaters with scattered metal nanodots are the suitable heating materials that can be applied for various functional devices.

KEYWORDS: transparent heaters, scattered metal nanodots, fluorine-doped tin oxide (FTO), thin films, saturated temperature



Thin transparent conductive films have been used widely for transparent heaters in various applications, such as military ground-based vehicles, periscopes, off-shore oil platforms, and electric vehicle windows. Heater materials that are optically transparent and electrically conductive, like graphene,^{1,2} single-walled and multiwalled carbon nanotubes (SWCNT/MWCNT),^{3–5} silver nanowires,⁶ Ga-doped zinc oxide,⁷ Cu wire networks,⁸ and indium tin oxide (ITO),^{9,10} have been studied recently. These materials are particularly intended to replace the incumbent ones, typically made of ITO, the price of which has doubled recently because of indium's scarcity and high demand. Moreover, ITO-based heaters have other disadvantages, such as intolerance to acid or base and are brittle under mechanical bending.²

As the substitution of ITO-based heating element, fluorine-doped tin oxide (SnO₂:F or "FTO") is a desirable candidate because of its excellent optical and electronic properties as an n-type semiconductor, with a wide bandgap of 3.6 eV, high carrier density, and low electrical resistivity. Moreover, it also has benefits as a defogger because of its thermal and chemical stabilities as well as being less expensive than indium-based materials.^{11–15} FTO can be manufactured by various techniques such as chemical vapor deposition,¹¹ spray pyrolysis,¹² sol–gel methods,¹³ and pulsed laser deposition.¹⁴ In this work, the fabrication of FTO thin films was carried out by electron cyclotron resonance–metal organic chemical vapor deposition (ECR-MOCVD). Advantages of ECR-MOCVD

versus the other methods include that it is possible to conduct the deposition at room temperature and no complex heating steps are required, like those generally conducted in the wet-based processing techniques, to remove water or other solvents. Thus, it is also possible to fabricate the transparent heater in a flexible polymer substrate, such as polyethylene terephthalate, without damaging the substrate properties.¹⁵

Metal nanoparticles are of great interest because of their important roles in different fields, including catalysis, optics, microelectronics, and sensors.¹⁶ Facile production and excellent optical and electronic properties of metal nanoparticles are other advantages for possible future applications.^{17,18} Taking these benefits into consideration, in this letter, we investigated the interfacial effects of three metal heating elements in the form of scattered metal nanodots—Cr, NiCr, and Ni—deposited on glass substrates, and in particular, their influences on the optical transmittance, electronic behavior, saturated temperature, thermal stability, and energy efficiency of FTO-based transparent heaters.

To fabricate high-performance FTO-based transparent heaters with scattered metal nanodots, we performed the experiments as illustrated in Scheme 1. This shows how the

Received: October 28, 2014

Accepted: December 31, 2014

Published: December 31, 2014

Scheme 1. Schematic Diagram of Fabrication of FTO-Based Transparent Heaters with Scattered Metal Nanodots Deposited on Pretreated Glass Substrate and the Heat-Cycle Experiment

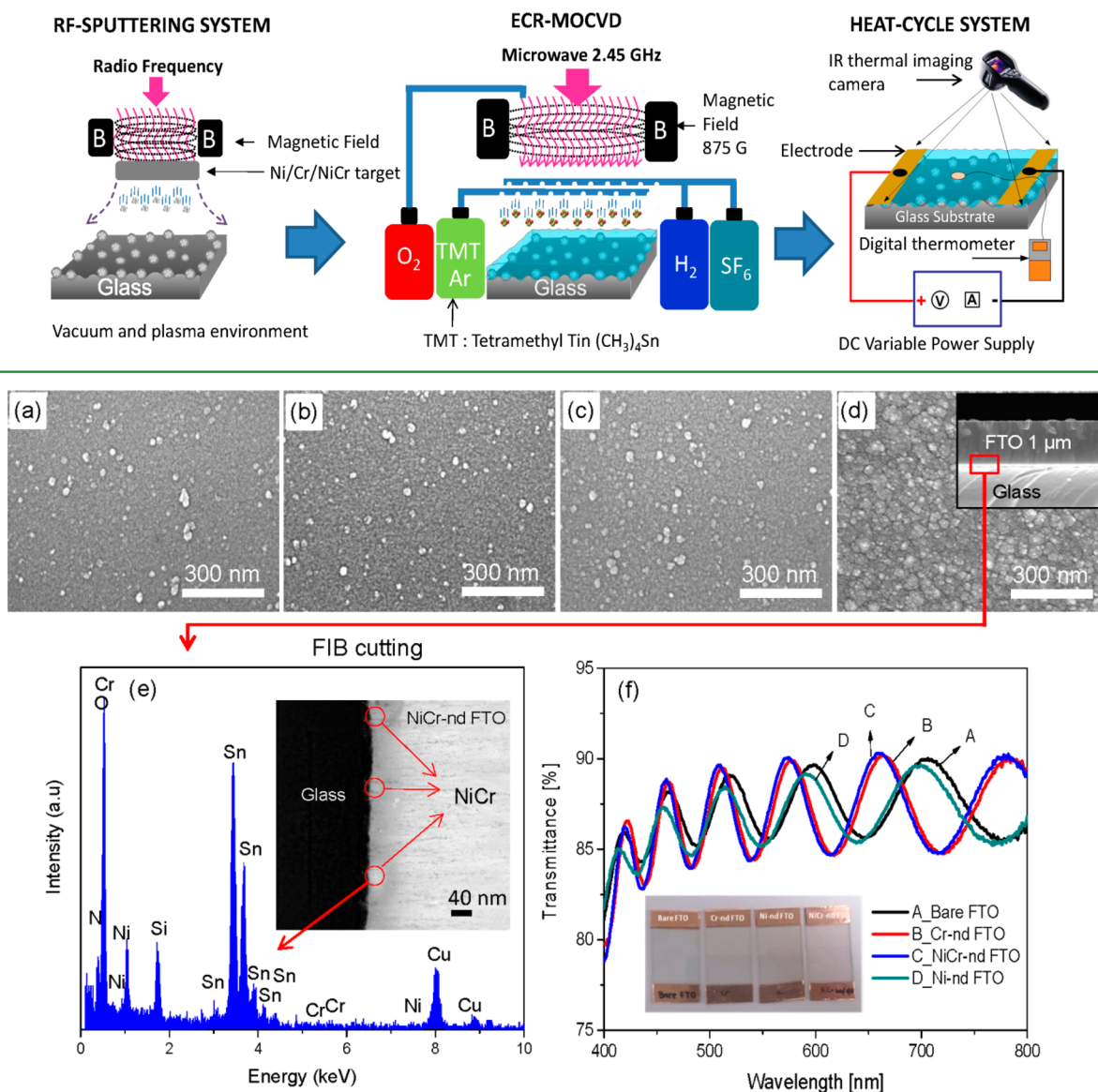


Figure 1. SEM images of as-deposited scattered metal nanodots on pretreated glass substrates (a) Ni-nd, (b) NiCr-nd, (c) Cr-nd, (d) NiCr-nd FTO and its cross-section in inset, (e) EDX analysis of NiCr-nd FTO from TEM and its cross-section image in inset, and (f) visible optical transmittance spectra of bare FTO, Cr-nd FTO, NiCr-nd, and Ni-nd FTO transparent heater and as-developed FTO transparent heaters with scattered metal nanodots in inset.

metal nanodots were grown on a pretreated glass surface, prepared by a plasma-enhanced sputtering system, the deposition of the FTO thin film carried out by ECR-MOCVD, and the apparatus constructed for the heat-cycle test. For the heat-cycle test, the copper tapes (5 mm × 25 mm) were attached at the edges of the transparent heater as current collectors and were connected to the DC power supply (see Supporting Information for experimental details).

Figure 1a–c show SEM images of as-deposited Ni-nd, NiCr-nd, and Cr-nd, respectively, on the pretreated glass substrate. We can observe the dispersed metal nanodots with particle sizes in the range of 10–30 nm. Once the FTO film is deposited, the presence of metal nanodots does not change the surface morphology of transparent heaters obviously, due to small amounts. Here, we provide a SEM image of the NiCr-nd

FTO and its cross-section (inset) in Figure 1d. The grain size of the FTO film is about 30–60 nm, with a thickness of 1 μm. To reveal the elemental composition of the transparent heater, and especially to demonstrate the existence of the scattered metal nanodots, we cut a cross-section of NiCr-nd FTO using a focused ion beam (FIB) method and observed it using energy-dispersive X-ray spectroscopy (EDX) in a TEM analysis, as shown in Figure 1e. Cr and Ni were confirmed to be present significantly, at energies of 0.5 and 1.5 keV, respectively. We also found considerable peaks for Sn at the energy range of 3–4.5 keV. The Si and Cu contributions to the spectrum are assumed to be due to the glass substrate and copper grid support during the measurement, respectively. Unfortunately we could not confirm the present of fluorine content as this element is easily decomposed by electron beam during the

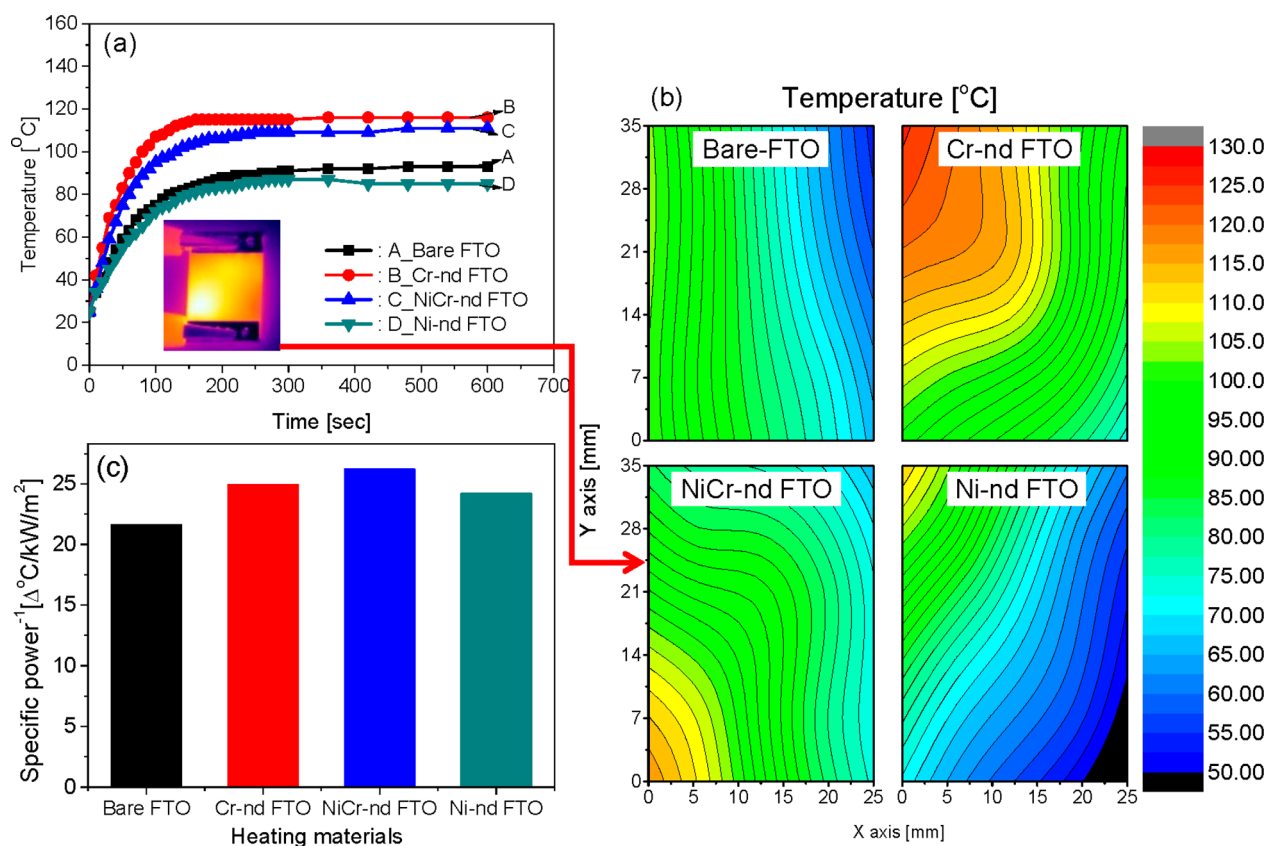


Figure 2. (a) Temperature profiles FTO-based transparent heaters with scattered metal nanodots energized by 12 V DC; (b) contour maps of temperature profiles of bare and FTO heaters with scattered metal nanodots (25 mm × 35 mm), powered by 12 V DC, which were captured during 10 min heat-cycle test. The 12 points were measured with coordinates at (5.5,7), (12.5,7), (19.5,7), (19.5,14), (12.5,14), (5.5,14), (5.5,21), (12.5,21), (19.5,21), (19.5,28), (12.5,28), and (5.5,28); (c) specific power of transparent heaters.

measurement. Furthermore, from the inset of Figure 1e we can see the particle size of NiCr-nd was ~30 nm, consistent with the SEM images. Figure 1f shows the optical transmission spectra of bare and metal nanodot FTO transparent heaters in the visible wavelength range (400–800 nm). At a wavelength of 550 nm, all samples exhibited optical transparency of more than 85%, which is favorable for a transparent conducting material. The corresponding values at this wavelength were 86, 85.1, 85.7, and 85.1% for bare, Cr-nd, NiCr-nd, and Ni-nd FTO heater, respectively (substrate subtracted). The slightly lower transmittance of the FTO heaters with scattered metal nanodots versus the bare one can be attributed to the absorption and scattering of visible light by the scattered nanodots inside the FTO films. Moreover, impurity phase compounds from the metal targets during sputtering may also cause such degradation, as observed previously.¹⁹

Because of safety and energy efficiency concerns, we investigated the heat-cycle of the transparent heaters with a relatively low applied voltage of 12 V DC. The relationship between the temperature changes over the time series powered by a constant voltage of 12 V measured at ambient conditions is shown in Figure 2a. The graph shows the surface temperature of the transparent heaters increased markedly over time until reaching the saturated point. Compared with other heater types, the Cr-nd FTO heater achieved the highest saturated temperature (116 °C) and the shortest response time (160 s) to obtain the steady-state point. The inclusion of Cr-nd in the FTO heater contributed to the outstanding thermal performance of the heaters, due to its excellent electrical properties,

such as lower sheet resistance (26.85 Ω/□), higher electrical (383 S cm⁻¹) and thermal (83 W m⁻¹ K⁻¹) conductivity (see the Supporting Information, Table S1). As the result, a faster transduction of electrical energy into Joule heating occurred, according to the relationship $P = V^2/R$ (where P is power [W], V is applied voltage [V], and R is resistance [Ω]).²

Despite the relatively low concentration of Cr particles in the NiCr-nd FTO (60% Ni, 40% Cr), the significant role of this heating element was further confirmed in boosting the thermal capabilities. In fact, the NiCr-nd FTO heater was the second highest saturated temperature (111 °C) followed by bare FTO (93 °C) and Ni-nd FTO (85 °C). The scattered metal nanodots also enhanced the thermal uniformity of FTO-based heaters, as captured by thermal imaging camera in Figure 2b. To distinguish the level of temperature uniformity, we applied the equation

$$T_{\text{UNI}} = [(T_{\text{MAX}} - T_{\text{MIN}})/2T_{\text{AVE}}]100\%$$

where T_{UNI} (%) is the temperature uniformity and T_{MAX} , T_{MIN} , and T_{AVE} are the highest, lowest, and average temperature (°C), respectively, measured at 12 points at the surface of the transparent heaters.¹⁵ The maps suggest the Cr-nd FTO heater shows the most uniform value (14.65%), followed by NiCr-nd FTO (19.2%), bare FTO (19.7%), and Ni-nd FTO (30%). The thermal uniformity of our FTO-based heaters seemed much better than that developed with a patterned wire,²⁰ a heater type commonly used to remove mist in conventional car windows today. This indicates that using our FTO-based transparent heaters in car windows could be the key to a faster

defogger. We also investigated the thermal stability of the FTO-based transparent heater by supplying a higher voltage, 16 V (see the Supporting Information, Figure S2a). A temperature overshoot was observed for the Cr-nd FTO heater until it reached the saturated point at 132 °C. We suggest an electrical breakdown mechanism was likely the reason for this case because the Cr-nd FTO heater with a relatively low electrical resistivity received a large amount of electrical energy in a certain period. As a consequence, some parts of the FTO thin film heater might have been broken, eventually increasing the electrical resistivity of the heater. The same phenomenon can be seen in the case of silver nanowire heaters.⁶ The NiCr-nd FTO heater showed a stable temperature profile during the heat-cycle test. We presume the Ni nanoparticles, in the form of the NiCr composite, balanced the Cr behavior at the higher voltage (see the Supporting Information, Figure S2b). The specific power of the FTO-based heater materials is presented in Figure 2c. The NiCr-nd FTO heater performed with the highest specific power of 26.2 °C m² kW⁻¹. This means that under a constant voltage, powering 1 kW m⁻² into this heater material will generate an additional increment of temperature of as much as 26.2 °C until achieving its saturation point at about 10 min. The specific power correlates closely with energy efficiency because it compares the output heat energy—represented by the temperature difference (ΔT) from the heater—and the input electric energy given by the DC power supply. Thus, in our study the most efficient transparent heater in terms of energy saving was NiCr-nd FTO, followed by Cr-nd FTO, Ni-nd FTO, and bare FTO.

It is also interesting to compare our FTO-based heaters with previously studied transparent heaters, such as those made with graphene,¹ AuCl₃-doped graphene,¹ MWCNT,⁴ SWCNT,³ and ITO.⁹ As displayed in Figure 3a, the Cr-nd FTO transparent heater showed superior saturated temperature, power density, and optical transmittance versus the other heaters with the same applied voltage of 12 V (see the Supporting Information, Table S2). To explain these phenomena, we provide an illustration in Figure 3b. Once a DC voltage is supplied through the copper electrodes at the edge of transparent heater, the electrons flow into the bulk of the FTO heater and pass through the scattered metal nanodots. Because the Ni, NiCr, and Cr nanodots are heating materials with relatively lower electrical resistivity, they are able to generate heat with higher temperature spots compared with the bulk films. The short distance among the metal nanodots, which is less than ~100 nm, helps create a uniform distribution of heat generated by the FTO heaters with the scattered metal nanodots. Like the other types of heaters, the heat-transfer mechanisms of the FTO-based transparent heater include three parameters: conduction, convection, and radiation. The conduction of heat dissipation takes place in the solid–solid interfaces, which are between scattered metal nanodots and the FTO layer, the scattered metal nanodots and the glass substrate, and the FTO film and the glass substrate. Convection and radiation heat transfers involve the surrounding air and FTO film surface.^{1,2} When a steady-state temperature is achieved, the heat loss is solely attributed to convection and radiation.

In conclusion, we investigated FTO-based transparent heaters with scattered Cr, NiCr, and Ni nanodots, prepared by a plasma-enhanced sputtering system and ECR-MOCVD. The heat-cycle tests demonstrated that with a low applied voltage, the Cr-nd FTO transparent heater showed the most efficient and stable performance, compared with bare FTO,

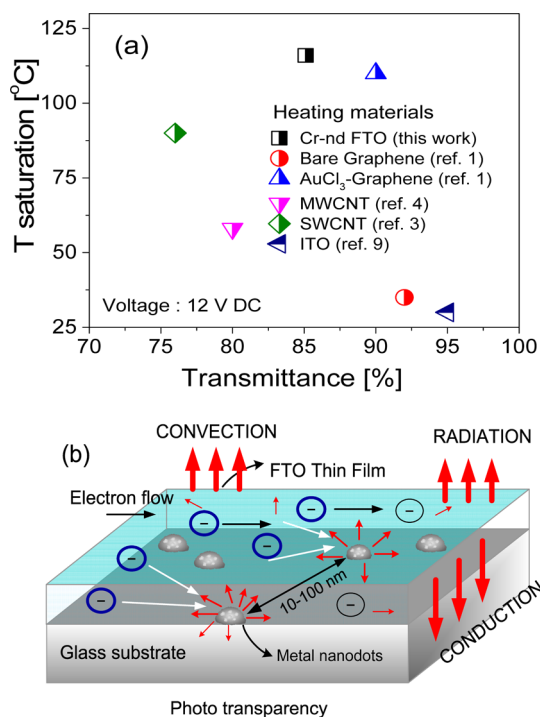


Figure 3. (a) Saturation temperature versus transmittance of Cr-nd FTO compared with other heating systems in the literature and (b) schematic illustration of heat generation and heat-transfer mechanisms of FTO transparent heaters with scattered metal nanodots.

NiCr-nd FTO, and Ni-nd FTO heaters. However, when a higher voltage was supplied, the Ni and Cr composite (NiCr-nd) FTO heater showed an excellent thermal response. This superior thermal performance was correlated with the low sheet resistance and high electronic performance of FTO-based heaters. Compared with bare graphene, MWCNT, SWCNT, and ITO-based heating systems, our FTO-based heaters indicate much better heat performances, especially in terms of optical transmittance, saturated temperature, and specific power density. These findings suggest that FTO transparent heaters with scattered metal nanodots may be useful for many functional devices including home appliances, military equipment, and other industrial applications.

■ ASSOCIATED CONTENT

📄 Supporting Information

Descriptions of experimental details for fabrication of FTO thin transparent heaters with scattered metal nanodots, electrical properties of the heaters, and a stability heat-cycle test in a higher voltage. This material is available free of charge via the Internet at <http://pubs.acs.org>.

■ AUTHOR INFORMATION

Corresponding Author

*E-mail: leejk@kist.re.kr and bijeon@shinhan.ac.kr.

Funding

This work was supported by Nano-Convergence Foundation (www.nanotech2020.org) funded by the Ministry of Science, ICT and Future Planning (MSIP, Korea) & the Ministry of Trade, Industry and Energy (MOTIE, Korea) [Project Name: Development of Functional Smart Film Manufacturing Technologies]. This work was also supported by KIST institutional program and research grants of NRF (NRF-

2012M1A2A2671792) funded by the National Research Foundation under the MSIP, Korea.

Notes

The authors declare no competing financial interest.

ACKNOWLEDGMENTS

The authors thank Mr. Joo Man Woo and Mr. Un Seok Kim for technical discussions during the study.

REFERENCES

- (1) Bae, J. J.; Lim, S. C.; Han, G. H.; Jo, Y. W.; Doung, D. L.; Kim, E. S.; Chae, S. J.; Huy, T. Q.; Luan, N. V.; Lee, Y. H. Heat Dissipation of Transparent Graphene Defoggers. *Adv. Funct. Mater.* **2012**, *22*, 4819–4826.
- (2) Sui, D.; Huang, Y.; Huang, L.; Liang, J.; Ma, Y.; Chen, Y. Flexible and Transparent Electrothermal Film Heaters Based on Graphene Materials. *Small* **2011**, *7*, 3186–3192.
- (3) Yoon, Y.-H.; Song, J.-W.; Kim, D.; Kim, J.; Park, J.-K.; Oh, S.-K.; Han, C.-S. Transparent Film Heater Using Single-Walled Carbon Nanotubes. *Adv. Mater.* **2007**, *19*, 4284–4287.
- (4) Jang, H. S.; Jeon, S. K.; Nahm, S. H. The Manufacture of a Transparent Film Heater by Spinning Multi-Walled Carbon Nanotubes. *Carbon* **2011**, *49*, 111–116.
- (5) Huang, Y. Y.; Terentjev, E. M. Transparent Electrode with a Nanostructured Coating. *ACS Nano* **2011**, *5*, 2082–2089.
- (6) Kim, T.; Kim, Y. W.; Lee, H. S.; Kim, H.; Yang, W. S.; Suh, K. S. Uniformly Interconnected Silver-Nanowire Networks for Transparent Film Heaters. *Adv. Funct. Mater.* **2013**, *23*, 1250–1255.
- (7) Ahn, B. D.; Oh, S. H.; Hong, D. U.; Shin, D. H.; Moujoud, A.; Kim, H. J. Transparent Ga-doped zinc oxide-based window heaters fabricated by pulsed laser deposition. *J. Cryst. Growth* **2008**, *310*, 3303–3307.
- (8) Kiruthika, S.; Gupta, R.; Rao, K. D. M.; Chakraborty, S.; Padmavathy, N.; Kulkarni, G. U. Large Area Solution Processed Transparent Conducting Electrode Based on Highly Interconnected Cu Wire Network. *J. Mater. Chem. C* **2014**, *2*, 2089–2094.
- (9) Im, K.; Cho, K.; Kwak, K.; Kim, J.; Kim, S. Flexible Transparent Heaters with Heating Films Made of Indium Tin Oxide Nanoparticles. *J. Nanosci. Nanotechnol.* **2013**, *13*, 3519–3521.
- (10) Ashida, T.; Miyamura, A.; Oka, N.; Sato, Y.; Yagi, T.; Taketoshi, N.; Baba, Y.; Shigesato, Y. Thermal Transport Properties of Polycrystalline Tin-Doped Indium Oxide Films. *J. Appl. Phys.* **2009**, *105*, 073909–1–073909–4.
- (11) Gao, K. H.; Lin, T.; Liu, X. D.; Zhang, X. H.; Li, X. N.; Wu, J.; Liu, Y. F.; Wang, X. F.; Chen, Y. W.; Ni, B.; Dai, N.; Chu, J. H. Low Temperature Electrical Transport Properties of F-Doped SnO₂ Films. *Solid State Commun.* **2013**, *157*, 49–53.
- (12) Premalal, E. V. A.; Dematage, N.; Kaneko, S.; Konno, A. Preparation of High Quality Spray-Deposited Fluorine-Doped Tin Oxide Thin Films Using Dilute di(n-butyl)tin(IV) Diacetate Precursor Solutions. *Thin Solid Films* **2012**, *520*, 6813–6817.
- (13) Senthilkumar, V.; Vickraman, P.; Ravikumar, R. Synthesis of Fluorine Doped Tin Oxide Nanoparticles by Sol–Gel Technique and Their Characterization. *J. Sol–Gel Sci. Technol.* **2010**, *53*, 316–321.
- (14) Kim, H.; Auyeung, R. C. Y.; Piqué, A. F-Doped SnO₂ Thin Films Grown on Flexible Substrates at Low Temperatures by Pulsed Laser Deposition. *Thin Solid Film* **2011**, *520*, 497–500.
- (15) Hudaya, C.; Park, J. H.; Lee, J. K. Effects of Process Parameters on Sheet Resistance Uniformity of Fluorine-Doped Tin Oxide Thin Films. *Nanoscale Res. Lett.* **2012**, *7*, 1–4.
- (16) Dai, X.; Wildgoose, G. G.; Salter, C.; Crossley, A.; Compton, R. G. Electroanalysis Using Macro-, Micro-, and Nanochemical Architectures on Electrode Surfaces. Bulk Surface Modification of Glassy Carbon Microspheres with Gold Nanoparticles and Their Electrical Wiring Using Carbon Nanotubes. *Anal. Chem.* **2006**, *78*, 6102–6108.
- (17) Maity, S.; Bochinski, J. R.; Clarke, L. I. Metal Nanoparticles Acting as Light-Activated Heating Elements within Composite Materials. *Adv. Funct. Mater.* **2012**, *22*, 5259–5270.
- (18) Maity, S.; Downen, L. N.; Bochinski, J. R.; Clarke, L. I. Embedded Metal Nanoparticles as Localized Heat Sources: An Alternative Processing Approach for Complex Polymeric Materials. *Polymer* **2011**, *52*, 1674–1685.
- (19) Liu, S.-J.; Chen, L.-Y.; Liu, C.-Y.; Fang, H.-W.; Hsieh, J.-H.; Juang, J.-Y. Physical Properties of Polycrystalline Cr-Doped SnO₂ Films Grown on Glasses Using Reactive DC Magnetron Co-sputtering Technique. *Appl. Surf. Sci.* **2011**, *257*, 2254–2258.
- (20) Baldasseroni, C.; Queen, D. R.; Cooke, D. W.; Maize, K.; Shakouri, A.; Hellman, F. Heat Transfer Simulation and Thermal Measurements of Microfabricated X-ray Transparent Heater Stages. *Rev. Sci. Instrum.* **2011**, *82*, 093904–1–093904–10.